

PHYSICAL REVIEW B

CONDENSED MATTER AND MATERIALS PHYSICS

THIRD SERIES, VOLUME 62, NUMBER 14

1 OCTOBER 2000-II

RAPID COMMUNICATIONS

Rapid Communications are intended for the accelerated publication of important new results and are therefore given priority treatment both in the editorial office and in production. A Rapid Communication in Physical Review B may be no longer than four printed pages and must be accompanied by an abstract. Page proofs are sent to authors.

X-ray-Raman scattering from the oxygen *K* edge in liquid and solid H₂O

D. T. Bowron,¹ M. H. Krisch,¹ A. C. Barnes,² J. L. Finney,³ A. Kaprolat,¹ and M. Lorenzen¹

¹European Synchrotron Radiation Facility, 6 rue Jules Horowitz, BP 220, 3804 Grenoble Cedex 09, France

²HH Wills Physics Laboratory, Royal Fort, Tyndall Avenue, Bristol BS8 1TL, United Kingdom

³Department of Physics and Astronomy, University College London, Gower Street, London, WC1E 6BT, United Kingdom

(Received 10 February 2000)

Inelastic x-ray scattering from oxygen 1s electrons in liquid and solid water were recorded up to 200 eV above the onset of the O *K* edge. The partial radial distribution function that characterizes the local environment of oxygen in the water/ice system was determined. Good agreement is found between the resulting partial distribution function for liquid water and that obtained from elastic neutron scattering. In the near-edge region distinct differences between the solid and liquid states are observed which arise from differences in the local structural and electronic environment of the oxygen atoms. The method thus promises a degree of insight into details of hydrogen bonding interactions.

I. Introduction. A number of experimental techniques are now available for obtaining high quality local atomic level structural information on increasingly complex liquid and glassy systems. Due to the absence of long-range structural order the most useful means of characterization is the interatomic partial pair distribution function. The most common techniques that allow us to probe these functions include isotopic substitution neutron-scattering methods,¹ extended x-ray absorption fine structure (EXAFS) spectroscopy,² and x-ray anomalous scattering.³ Due to various experimental constraints, these techniques are difficult to apply to investigations of the local atomic environment of carbon and oxygen, two particularly important atoms in a large range of chemically and biologically important systems.

Traditionally, the most powerful probe of interatomic and intermolecular structural correlations in liquid systems has been neutron scattering with isotopic substitution. That technique exploits the fact that isotopes of the elements often have significantly different neutron-scattering cross sections and in those cases it becomes possible to extract pair distribution functions centered on the isotopically substituted element.¹ Unfortunately two of the most important light elements, carbon and oxygen, do not possess isotopes with sufficiently different scattering cross sections for the technique to be usefully applicable. The x-ray analog of this technique

is x-ray anomalous scattering, where the variation in the atomic scattering cross section is obtained by tuning the incident photon energy to be close to a core electron absorption resonance.³ A third technique is EXAFS spectroscopy, which again makes use of the core electron x-ray absorption resonances.² For the light elements such as carbon and oxygen, the 1s absorption thresholds are 284 eV and 543 eV, respectively. At these energies there are formidable technical challenges in the design of a sample environment such as the general requirement for high vacuum which is largely incompatible with measurements of the liquid state. Measurements of the oxygen x-ray absorption spectra in water and ice have been attempted by a number of other techniques, e.g., x-ray fluorescence⁴ and photoelectron yield,⁵ with the aim of extracting structural information. However, detailed structural analysis proved unconvincing as to intermolecular bond distances or remained unattempted due to the significant experimental difficulties faced.

These challenges can be circumvented in an x-ray-Raman scattering (XRS) experiment. Here the energy required to excite a core electron is provided by an *inelastically* scattered x-ray photon.⁶ If the momentum transfer involved in the inelastic scattering process is small compared to the inverse of the radial extent of the core electron wave function r ($Qr \ll 1$), the obtained spectrum is analogous to that of a

soft x-ray measurement.⁷ This contrasts with conventional soft x-ray absorption measurements where the required energy is provided directly by absorption of the incident x-ray photon. Thus, in the case of XRS there is significant freedom in the choice of the incident photon energy which frees us from the aforementioned sample environment limitations. Following the phenomenon's initial observation, a handful of studies have demonstrated the correspondence between the x-ray-Raman excited spectrum and the direct soft x-ray absorption spectrum of crystalline low-*Z* elements.^{8,9} However, to date, a full detailed analysis of such spectra in terms of modern x-ray absorption theory and methodology has been absent.

In this paper we present x-ray-Raman data for liquid water at 293 K and for polycrystalline ice Ih at 265 K. The water and ice system offers a number of advantages for establishing the viability of the technique as a probe of local structural and electronic correlations of both ordered and disordered light atom systems. For example, as the structures of both ice Ih and liquid water have been reliably probed by many other techniques including neutron and x-ray diffraction,^{10,11} high quality structural data are available for validation. In addition, the subtleties of the interatomic and intermolecular interactions in water and ice, in particular the fundamentally important phenomenon of hydrogen bonding, are still not comprehensively understood¹² and many pertinent scientific questions remain to be answered. Due to the wide relevance of aqueous systems to many important areas of physics, chemistry, and biology, a detailed understanding of the hydrogen bond is of fundamental importance. A method capable of giving detailed structural and electronic information on hydrogen bonding in disordered systems is thus potentially very useful.

II. Experiment. The experiment was performed on the Inelastic Scattering Beamline II (ID28) at the European Synchrotron Radiation Facility. The incident linearly polarized x rays produced by a 35 mm undulator were monochromatized by a cryogenically cooled silicon (111) double crystal monochromator, providing an energy bandwidth of approximately 1.5 eV. The scattered photons were energy analyzed in the horizontal plane by a Si(660) spherical crystal in backscattering geometry at a fixed energy of 9686 eV while the energy transfer was tuned through the oxygen *K* edge by scanning the Si(111) monochromator from 10 200 eV to 10 400 eV. In order to avoid strong variations in the incident photon beam intensity, the undulator gap was changed every 30 eV with a typical step size of 20 μm . The incident beam intensity in front of the sample was monitored by a silicon diode, recording the signal arising from air scattering. The inelastic scattering signal was observed at 50° within a solid angle of about 3.6 mrad². The scattering angle of 50° corresponds to a momentum transfer Q of 4.38 \AA^{-1} at 10 229 eV, where the oxygen *K* edge was observed. The radial extent of the oxygen 1s wave function is approximately 0.07 \AA , which corresponds to a momentum transfer–radial wave function product $Qr=0.29$. This choice insures that the excitation process is largely dominated by electric dipole transitions, whereas monopole and quadrupole transition strengths are much weaker.¹³ The overall experimental resolution was 2 eV.

In Fig. 1 we present a logarithmically scaled overview plot of the detected signal intensity as a function of the inci-

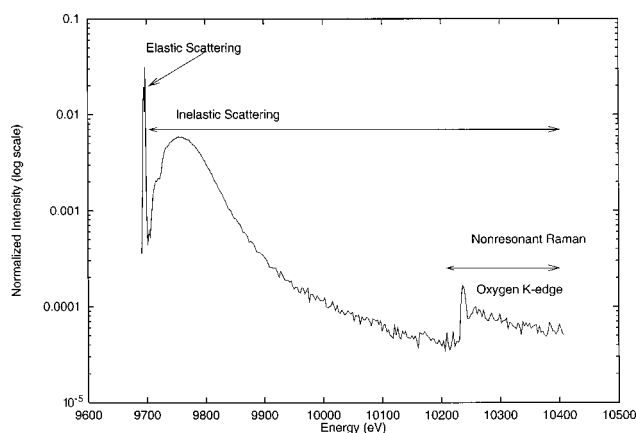


FIG. 1. Overview plot of the relative strengths of the elastic, Compton, and nonresonant Raman processes in ice, shown on a logarithmic scale. The useful statistical data collection rate of the nonresonant Raman process corresponds to approximately 60 Hz.

dent x-ray energy. For each sample, several spectra were recorded and summed together to correspond to a total data acquisition time of 24 h.

III. Results. Figure 2 shows the measured XRS spectra for liquid water and ice Ih as a function of energy transfer. The spectra have been obtained by subtracting a constant background as determined on the energy gain side about 20 eV below the maximum of the elastic line. Then the monotonically decreasing tail of the valence electron $S(Q, \omega)$ was fitted with an exponential function where the weak energy dependence of the inelastic cross section⁶ was taken into account. Both spectra are characterized by a strong absorption resonance which is followed by a broader absorption feature at 565 eV. The ice spectrum is slightly stronger than that of the liquid, which is a natural consequence of the higher degree of structural order in the crystal. The inset enlargement of the absorption edge reveals a distinct difference in the shape of the edge resonance between the liquid and solid states. In both states, the absorption edge appears to consist of at least two components, but of differing spectral weight. In a simplistic model, these can be assigned to electric dipolar transitions from the 1s core state of the oxygen atom to the lowest unoccupied molecular orbitals of π^* and σ^* symmetry, which following the base molecular symmetry are known to be centered along the O-H vector of the water molecule.^{14–16} This region of an absorption spectrum is highly sensitive to the electronic and bonding environment of the absorbing species but an unambiguous deconvolution of the structural and electronic contributions to the spectra still remains a nontrivial problem.

The analysis of the data was pursued using modern EXAFS spectroscopy analytic methods, developed specifically to handle many of the subtleties of liquid state analysis.^{17,18} In particular we have adopted the recently developed technique of refining the liquid state data while constraining the analysis to known physical constraints of the bulk density and isothermal compressibility of water.¹⁹ Such analyses contain a number of free parameters that govern the reliability of the distance and coordination number evaluation. These parameters can only be reliably determined by reference to a well-characterized structural system such as a

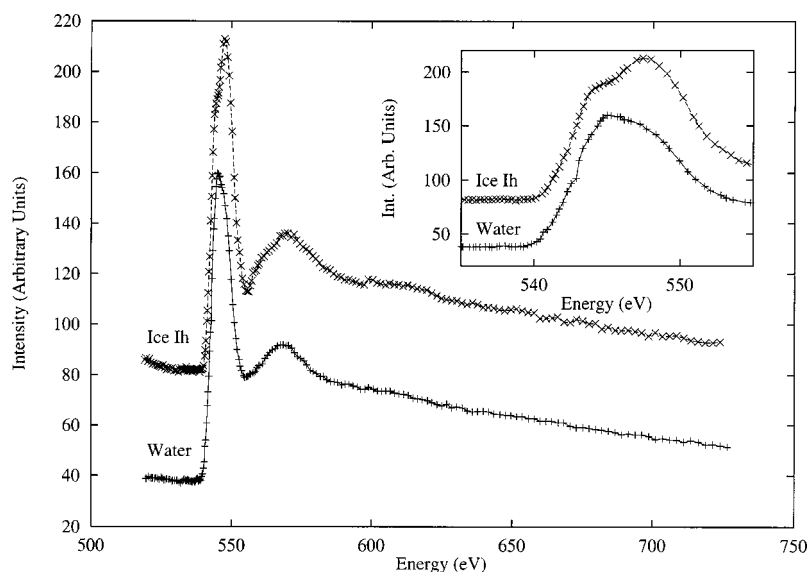


FIG. 2. The oxygen K absorption edge as measured by x-ray-Raman scattering for ice Ih ($\times\times\times$) and liquid water ($+++$). The overall counting time per point was 300 s for water and 540 s for ice.

crystal. In this respect the water/ice system is an almost ideal case since the short-range structure of ice Ih is well known from crystallographic measurements and can be used to calibrate the liquid state data. We therefore analyzed the data of ice Ih and extracted the parameters that govern the calibration of the interatomic distance scale and coordination numbers. These calibrated parameters were subsequently transferred to the refinement of the liquid state structure.

During the analysis of the ice data, it was found essential to include the spectral contribution to the absorption signal that arises from the intramolecular and intermolecular hydrogen atoms. This inclusion of the hydrogen contribution is particularly important since the electronic scattering potential for hydrogen is, at $1/8$ that of the oxygen, significant. Additionally, the approximately collinear O-H-O atomic arrangement of ice Ih results in the hydrogens being in a “focusing” configuration for the oxygen-oxygen correlations. Data refinement in the absence of these hydrogen contributions persistently led to unphysical values for the interatomic

distance scale calibration parameter and signal amplitude scaling factor. Such inconsistencies were reflected in the theoretically expected energy for the onset of the absorption edge and the coordination numbers, respectively. Following the inclusion of hydrogen atom contributions, the data refined reliably, with the energy zero determined as 543 eV.

An additional spectral component found to be important in modeling the ice and water absorption spectra was the inclusion of an arctangent discontinuity in the absorption spectrum background at ~ 20 eV above the edge onset energy. This component allowed for the presence of a parasitic secondary electron excitation of the oxygen $2s$ electron. Such double electron excitation effects are often important considerations in the analysis of conventionally collected x-ray absorption data.²⁰ As with the other calibration parameters, once determined for the known solid-state ice data, it was transferred unvaried to the liquid state analysis. This is justified because the local chemical environment of the oxygen atom is considered similar between the two systems.

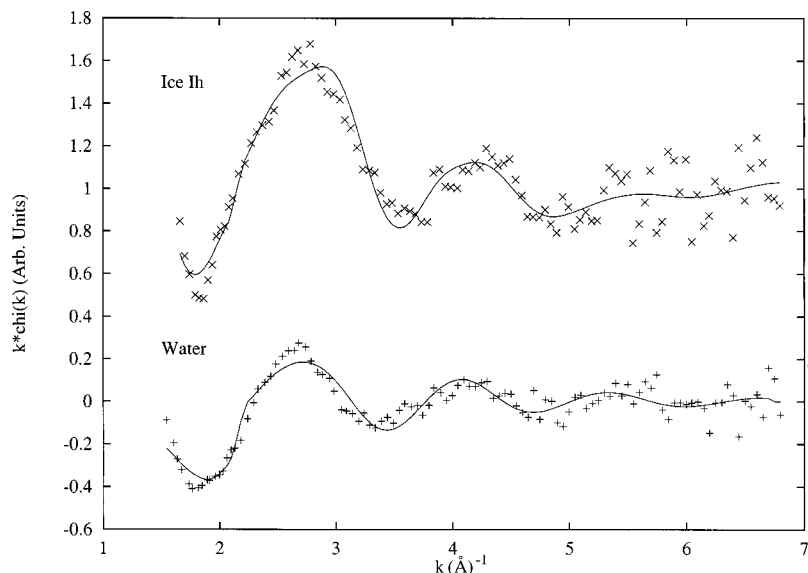


FIG. 3. The $k\chi(k)$ weighted spectra for ice Ih and water and model fits to the data. $\chi(k)$ is defined as $(\mu - \mu_0)/\mu_0$ where μ is the measured atomic absorption cross section for a condensed matter state and μ_0 is the single atomic absorption background; k is the magnitude of the photoelectron momentum wave vector, given by the well-known relationship $E = \hbar^2 k^2 / 2m_e$ where m_e is the electron mass.

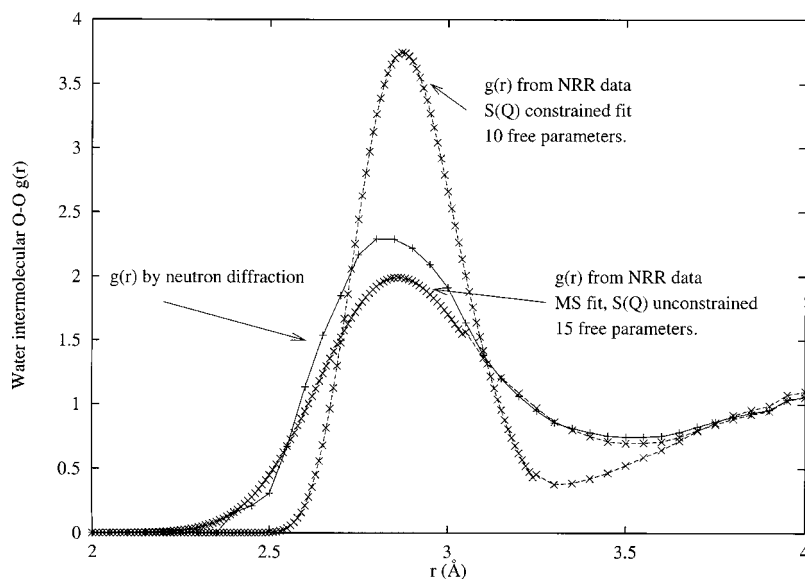


FIG. 4. The oxygen-oxygen partial pair distribution function as determined by neutron scattering (+++) (Ref. 21), and XRS (×××). The two XRS functions illustrate the range of structural models that were found to be consistent with the collected data. We note in particular, the consistency between the three curves in the determined intermolecular O-O distance.

Figure 3 shows the results of the data refinement for both the solid and liquid state systems. Figure 4 gives the resulting partial distribution function of water oxygen atom-pair correlations in the liquid, and comparison of the XRS results with those obtained from isotopic substitution neutron-scattering methods.²¹ The range of model local structures that can satisfactorily fit the XRS data is illustrated by the upper and lower curves. These models are (i) an unconstrained fit to the local environment, in which no attempt is made to satisfy the known long-range structural characteristics such as bulk density (lower XRS fit), and (ii) a more highly constrained model in which the macroscopic bulk density and isothermal compressibility are constrained to the values known for water (upper XRS fit). This data analysis method is generally found to position more accurately the onset of the radial distribution function, which is often the most problematic task in neutron diffraction and conventional x-ray absorption spectroscopy analyses. Within the constraints imposed by the statistical quality of the data (Fig. 1), it is difficult to unambiguously distinguish between the two models. However, we note that it is possible to reliably determine the short-range interatomic distances between light atoms in structurally disordered systems by a chemically specific x-ray technique. The first neighbor oxygen-oxygen distance was found to peak consistently at a value of 2.87 Å. As always with x-ray absorption spectroscopy analyses, the determination of the coordination number is more difficult. The obtained values range between 4 (unconstrained) and 7 (constrained) and are consistent with the neutron results within the limits of the experimental data quality. Improvements in the counting statistics that are within the range of the current experimental capabilities will significantly improve our ability to reduce this uncertainty.

In the above analysis, we have focused attention on the signal beyond a k value of 1.6 \AA^{-1} . This is for two principal reasons: (1) The increasing importance of multiple scattering contributions as one approaches the absorption edge region combined with (2) the considerable difficulty in defining a

reliable set of atomic potentials in which the electron scattering and atomic excitation processes take place.

Some of the challenges that remain to be faced in the analysis of the near-edge light element absorption spectra are the following: (1) The large core hole excited-state lifetime which correlates with a large coherence lifetime for the free, propagating electron. There is hence a considerable scattering volume for single and multiple scattering phenomena that must be considered. (2) The local asphericity of the scattering potentials, in both the molecular and atomic framework, as well as the poor approximation to the excited state potentials.

IV. Conclusions. These experiments on the ice/water system demonstrate the potential of the x-ray-Raman technique in combination with state of the art x-ray absorption spectroscopy analysis methods, to address questions relating to local structure around light elements, typically between helium and aluminum. The technique thus has potentially enormous possibilities for investigations of structure and bonding in a range of chemical, biological, and materials science. The key points that we highlight here, in particular for aqueous systems, are the following: (1) The resulting partial distribution function we obtain for liquid water, centered on the oxygen, is in good agreement with commonly accepted results. (2) The use of high-energy x-ray photons enables studies under a wide range of experimental conditions, for example high pressure and high temperature. (3) The possibility, albeit given theoretical developments, to give insight into the details of hydrogen bonding interactions through two routes: (a) the sensitivity of the absorption threshold to the bonding and electronic environment of oxygen, and (b) the hydrogen contributions to the structural components of the spectra.

We thank D. Gambetti, B. Gorges, K. Martel, and J. F. Ribois for technical assistance and commissioning of the ESRF beamline ID28 and the U.K. Engineering and Physical Sciences Research Council Liquid Matter Network for support and scientific stimulus.

- ¹J. E. Enderby and G. W. Neilson, in *Water: A Comprehensive Treatise*, edited by F. Franks (Plenum, New York, 1979).
- ²D. E. Sayers, *et al.*, Phys. Rev. Lett. **27**, 1024 (1971).
- ³P. H. Fuoss *et al.*, Phys. Rev. Lett. **46**, 1537 (1981).
- ⁴B. X. Yang and J. Kirz, Phys. Rev. B **36**, 1361 (1987).
- ⁵R. A. Rosenberg *et al.*, Phys. Rev. B **28**, 3026 (1983).
- ⁶T. Suzuki, J. Phys. Soc. Jpn. **22**, 1139 (1967).
- ⁷Y. Mizuno and Y. Ohmura, J. Phys. Soc. Jpn. **22**, 445 (1967).
- ⁸K. Tohji and Y. Udagawa, Phys. Rev. B **36**, 9410 (1987).
- ⁹H. Nagasawa *et al.*, J. Phys. Soc. Jpn. **58**, 710 (1989).
- ¹⁰A. K. Soper *et al.*, J. Chem. Phys. **106**, 247 (1997).
- ¹¹W. F. Kuhs and M. Lehmann, Water Sci. Rev. **2**, 1 (1985).
- ¹²E. D. Isaacs *et al.*, Phys. Rev. Lett. **82**, 600 (1999).
- ¹³H. Nagasawa *et al.*, J. Phys. Soc. Jpn. **66**, 3139 (1997).
- ¹⁴C. J. Ballhausen and H. B. Gray, in *Molecular Orbital Theory* (W. A. Benjamin Inc., New York, 1964).
- ¹⁵G. Pastori Parravicini and L. Resca, Phys. Rev. B **8**, 3009 (1973).
- ¹⁶W. L. Jorgensen and L. Salem, *The Organic Chemists Book of Orbitals* (Academic Press, New York, 1973).
- ¹⁷A. Filipponi *et al.*, Phys. Rev. B **52**, 15 122 (1995).
- ¹⁸A. Filipponi and A. Di Cicco, Phys. Rev. B **52**, 15 135 (1995).
- ¹⁹A. Filipponi, J. Phys.: Condens. Matter **6**, 8415 (1994).
- ²⁰A. Di Cicco *et al.*, Phys. Rev. B **54**, 9086 (1996).
- ²¹Data kindly provided by M. A. Ricci (Università di Roma Tre, Dipartimento di Fisica E. Amaldi, V. Della Vasca Navale 84, Roma, 00146, Italy) and A. K. Soper (ISIS Division, Rutherford Appleton Laboratory, Chilton, Didcot, Oxon, OX11 0QX, U.K.).